

Oscillatory instability in a driven granular gas

EVGENIY KHAIN and BARUCH MEERSON

Racah Institute of Physics, Hebrew University of Jerusalem, Jerusalem 91904, Israel

PACS. 45.70.-n – Granular systems.

PACS. 45.70.Qj – Pattern formation.

Abstract. – We discovered an oscillatory instability in a system of inelastically colliding hard spheres, driven by two opposite “thermal” walls at zero gravity. The instability, predicted by a linear stability analysis of the equations of granular hydrodynamics, occurs when the inelasticity of particle collisions exceeds a critical value. Molecular dynamic simulations support the theory and show a stripe-shaped cluster moving back and forth in the middle of the box away from the driving walls. The oscillations are irregular but have a single dominating frequency that is close to the frequency at the instability onset, predicted from hydrodynamics.

Introduction. – Granular gas - a system of inelastically colliding hard spheres - is a minimalistic model of granular flow that has received much recent attention [1]. In particular, this model captures *clustering*, a generic and fascinating phenomenon in rapid granular flows resulting from the collisional loss of the kinetic energy of random motion of particles. The formation and structure of granular clusters have been investigated in many works, both in the context of a freely “cooling” granular gas [2] and for driven granular gases [3, 4, 5, 6, 7, 8, 9, 10, 11, 12, 13, 14, 15, 16, 17, 18]. The basic physics of clustering can often be described in a hydrodynamic language, in terms of a collective condensation mode driven by bulk losses of energy. Similar condensation processes, driven by *radiative* energy losses in gases and plasmas, have been known for a long time [19]. A complete understanding of the properties of granular gas (a system intrinsically far from equilibrium) is still lacking. One important open question is the exact criteria for the validity of kinetic theory and Navier-Stokes hydrodynamics, developed in the 80-ies [20, 21].

Driven granular gas has the advantage that a steady state is achievable: the energy supplied into the system can be balanced by the collisional energy losses. We have focused in this work on a simple model: inelastic smooth hard spheres confined in a rectangular box and driven by two opposite “thermal” walls at zero gravity. Prototypical granular systems of this type were considered by many workers. In the early work, theoretical [5, 8, 10] and experimental [4], the “stripe state”: a denser and “colder” stripe-like cluster of particles, away from the driving wall(s), was documented. The formation of the stripe state has a simple explanation. Due to the inelastic particle collisions, the granular temperature goes down with an increase of the distance from the thermal wall(s). To maintain the steady-state pressure balance, the particle density should increase with this distance. For a large density contrast, the stripe state is observed.

It has been found more recently that the stripe state is only one, trivial state of this system. In a certain region of parameters the stripe state becomes either unstable or metastable and undergoes a spontaneous symmetry breaking and phase separation. As the result, a higher-density "phase" coexists with a lower-density phase in the direction *parallel* to the driving wall(s) [11, 12, 13, 15, 16, 17, 14]. A fascinating phenomenology of this far-from-equilibrium phase separation, and analogy with van der Waals gas [14] put this system into a list of pattern-forming systems far from equilibrium.

In this work we report a new and very different symmetry-breaking instability in the same system. Like the phase separation instability, the new instability occurs when the inelasticity $q = (1 - r)/2$ exceeds a critical value depending on the rest of the parameters of the system (here r is the coefficient of normal restitution of the particle collisions). In contrast to the phase separation instability, this is an instability in the direction *normal* to the driving wall(s), and it is oscillatory. As it develops, the stripe-shaped cluster in the middle of the system exhibits large irregular oscillations with a single dominating frequency.

The rest of the paper is organized as follows. First, we formulate a hydrodynamic model and briefly describe the static stripe state. Then we present a linear hydrodynamic stability analysis of the stripe state that predicts oscillatory instability. The instability is then observed in molecular dynamic (MD) simulations. Finally, we briefly discuss our results.

Model and static stripe state. – Let $N \gg 1$ identical smooth hard disks with diameter d and mass m move and inelastically collide inside a two-dimensional rectangular box with width L and height H . There is no gravity in the model. The system is driven by two thermal walls, with the same temperature T_0 , located at $x = -L/2$ and $x = L/2$. We assume nearly elastic particle collisions, $q \ll 1$, and moderate granular densities: $n/n_c \leq 0.5$, where n is the local number density of the particles, and $n_c = 2/(\sqrt{3}d^2)$ is the hexagonal dense packing density. These assumptions enable us to employ a standard version of Navier-Stokes granular hydrodynamics [21]. Hydrodynamics is expected to be valid when the mean free path of the particles is much smaller than any length scale (and the mean time between two consecutive collisions is much smaller than any time scale) described hydrodynamically. Let us measure the distance in the units of L , the time in the units of $L/T_0^{1/2}$, the density $n(\mathbf{r}, t)$ in the units of n_c , the granular temperature $T(\mathbf{r}, t)$ in the units of T_0 , and the mean velocity $\mathbf{v}(\mathbf{r}, t)$ in the units of $T_0^{1/2}$. Then the hydrodynamic equations [21, 22] become dimensionless:

$$\begin{aligned} dn/dt + n \nabla \cdot \mathbf{v} &= 0, & n d\mathbf{v}/dt &= \nabla \cdot \mathbf{P}, \\ n dT/dt + p \nabla \cdot \mathbf{v} &= \epsilon \nabla \cdot (T^{1/2} F_1 \nabla T) - \epsilon R n G T^{3/2}. \end{aligned} \quad (1)$$

Here $\mathbf{P} = [-p + \epsilon n G T^{1/2} \text{tr}(\mathbf{D})] \mathbf{I} + \epsilon F_2 T^{1/2} \hat{\mathbf{D}}$ is the stress tensor, $p = nT(1 + 2G)$ is the equation of state, $\mathbf{D} = (1/2) [\nabla v + (\nabla v)^T]$ is the rate of deformation tensor, $\hat{\mathbf{D}} = \mathbf{D} - (1/2) \text{tr}(\mathbf{D}) \mathbf{I}$ is the deviatoric part of \mathbf{D} , and \mathbf{I} is the identity tensor. The functions F_1 and F_2 are the following:

$$F_1 = nG \left[1 + \frac{9\pi}{16} \left(1 + \frac{2}{3G} \right)^2 \right] \quad \text{and} \quad F_2 = nG \left[1 + \frac{\pi}{8} \left(1 + \frac{1}{G} \right)^2 \right],$$

where

$$G = \frac{\pi n}{2\sqrt{3}} \frac{\left(1 - \frac{7\pi n}{32\sqrt{3}} \right)}{\left(1 - \frac{\pi n}{2\sqrt{3}} \right)^2}.$$

The two scaled parameters entering Eqs. (1) are the small parameter $\epsilon = 2\pi^{-1/2}d/L \ll 1$ and the parameter $R = (16/\pi)(1-r)\epsilon^{-2}$ that shows the relative role of the collisional heat loss and heat conduction. The boundary conditions for the temperature become $T(x = -1/2, y, t) = T(x = 1/2, y, t) = 1$. For the velocity we demand zero normal components and slip (no stress) conditions at all boundaries. We assume that H is small enough, so that no symmetry breaking can occur in the y -direction [11, 12, 13]. Therefore, the hydrodynamic variables are independent of y , while the mean flow, if any, is directed along the x -axis. The conservation of the total number of particles yields $\int_{-1/2}^{1/2} dx n(x, t) = f$, where $f = N/(LHn_c)$ is the average area fraction of the grains, an additional scaled parameter of the problem.

The static stripe state is described by the equations

$$[n_s T_s (1 + 2G_s)]' = 0 \quad \text{and} \quad (T_s^{1/2} J_1 T_s')' = R n_s G_s T_s^{3/2}, \quad (2)$$

where $G_s = G(n_s)$, $J_1 = F_1(n_s)$, and the primes denote the x -derivatives. Figure 1a shows an example of the temperature and density profiles of this state. Notice that, despite the presence of relatively large temperature and density gradients in the stripe state, the mean free path of the particles remains, at $q \ll 1$, much smaller than the characteristic length scale of these gradients [5]. Therefore, hydrodynamics remains valid.

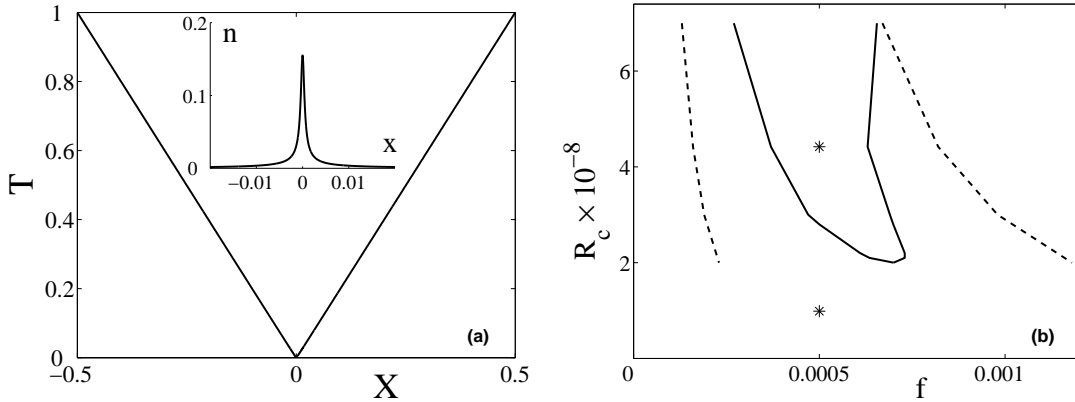


Fig. 1 – (a) – The scaled temperature profile of the static stripe state for $R = 4.42 \cdot 10^8$ and $f = 0.00063$. The inset shows the respective density profile. Except in a small vicinity of $x = 0$, the gas is dilute in this example. As the result, the scaled temperature profile there is $T \simeq 2|x|$, as follows from the dilute limit of Eqs. (2). (b) – The solid line is the oscillatory instability threshold $R = R_c$ versus the average area fraction f at $\epsilon = 4 \cdot 10^{-5}$. The instability occurs when $R > R_c$. The dashed lines show the borders of the spinodal interval of the phase separation instability that develops in the same system at large enough H . The two asterisks correspond to two MD simulations (see Figs. 2 - 4).

Linear stability analysis. – The linear stability analysis involves linearization of Eqs. (1) around the static profiles $n_s(x)$ and $T_s(x)$. We substitute

$$n(x, t) = n_s(x) + e^{-i\omega t} \nu(x), \quad T(x, t) = T_s(x) + e^{-i\omega t} \Theta(x), \quad \text{and} \quad v(x, t) = e^{-i\omega t} \psi(x), \quad (3)$$

where $\text{Im } \omega > 0$ (< 0) corresponds to growth (damping) of the small perturbation, and obtain the linearized equations:

$$-i\omega\nu + (n_s\psi)' = 0,$$

$$\begin{aligned}
& -i\omega n_s \psi = -(n_s(1+2G_s)\Theta)' - (T_s J_3 \nu)' + \epsilon \left(T_s^{1/2} n_s G_s \psi' \right)' + \frac{\epsilon}{2} \left(T_s^{1/2} J_2 \psi' \right)', \\
& -i\omega n_s \Theta + n_s \psi T_s' + n_s T_s (1+2G_s) \psi' \\
& = \epsilon \left[\left(T_s^{1/2} \Theta \right)' J_1 \right]' + \epsilon \left(T_s^{1/2} T_s' J_4 \nu \right)' - \epsilon R \left(\frac{3}{2} T_s^{1/2} n_s G_s \Theta + T_s^{3/2} J_5 \nu \right), \tag{4}
\end{aligned}$$

where $J_2 = F_2(n_s)$, $J_3 = 1 + 2G_s + 2n_s dG_s/dn_s$,

$$J_4 = \frac{1}{16G_s} [4\pi + 12\pi G_s + (16 + 9\pi)G_s^2] + \frac{n_s}{16G_s^2} [-4\pi + (16 + 9\pi)G_s^2] \frac{dG_s}{dn_s},$$

$J_5 = G_s + n_s dG_s/dn_s$ and $dG_s/dn_s = (9\pi/4)(16\sqrt{3} + \pi n_s)(6 - \sqrt{3}\pi n_s)^{-3}$. Eliminating $\nu(x)$ from equations (4), we arrive at a linear eigenvalue problem for the two-component eigenvector $\mathbf{U}(x) = [\psi(x), \Theta(x)]$, corresponding to the complex eigenvalue ω :

$$\mathbf{A} \mathbf{U}'' + \mathbf{B} \mathbf{U}' + \mathbf{C} \mathbf{U} = 0. \tag{5}$$

The elements of matrices \mathbf{A} , \mathbf{B} and \mathbf{C} are

$$\begin{aligned}
A_{11} &= -(n_s/i\omega) T_s J_3 + \epsilon a_0 n_s G_s + (\epsilon/2) a_0 J_2, & A_{21} &= \epsilon (n_s/i\omega) T_s^{1/2} T_s' J_4, \\
A_{12} &= 0, & A_{22} &= \epsilon a_0 J_1, \\
B_{11} &= -(n_s/i\omega) T_s' J_3 - (n_s/i\omega) T_s n_s' J_6 - (2n_s'/i\omega) T_s J_3 + \epsilon a_1 n_s G_s + \epsilon a_0 n_s' J_5 \\
&\quad + (\epsilon/2) a_1 J_2 + (\epsilon/2) a_0 n_s' J_7, \\
B_{21} &= -n_s T_s (1+2G_s) + \epsilon (n_s/i\omega) (T_s^{1/2} T_s')' J_4 + \epsilon (n_s/i\omega) T_s^{1/2} T_s' n_s' J_8 \\
&\quad + \epsilon (2n_s'/i\omega) T_s^{1/2} T_s' J_4 - \epsilon R (n_s/i\omega) T_s^{3/2} J_5, \\
B_{12} &= -n_s (1+2G_s), & B_{22} &= 2\epsilon a_1 J_1 + \epsilon a_0 n_s' J_4, \\
C_{11} &= i\omega n_s - (n_s'/i\omega) T_s' J_3 - ((n_s'')^2/i\omega) T_s J_6 - (n_s''/i\omega) T_s J_3, \\
C_{21} &= -n_s T_s' + \epsilon (n_s'/i\omega) (T_s^{1/2} T_s')' J_4 + \epsilon (n_s'/i\omega) T_s^{1/2} T_s' n_s' J_8 \\
&\quad + \epsilon (n_s''/i\omega) T_s^{1/2} T_s' J_4 - \epsilon R (n_s'/i\omega) T_s^{3/2} J_5, \\
C_{12} &= -n_s' J_3, & C_{22} &= i\omega n_s + \epsilon a_2 J_1 + \epsilon a_1 n_s' J_4 - (3/2) \epsilon R n_s G_s T_s^{1/2}, \tag{6}
\end{aligned}$$

and

$$\begin{aligned}
J_6 &= 4 dG_s/dn_s + 2 n_s d^2 G_s/dn_s^2, \\
J_7 &= (1/8) G_s^{-1} [\pi + 2\pi G_s + (8 + \pi)G_s^2] + (1/8) G_s^{-2} n_s [-\pi + (8 + \pi)G_s^2] dG_s/dn_s, \\
J_8 &= (\pi/2) G_s^{-3} n_s (dG_s/dn_s)^2 - (\pi/4) G_s^{-2} (2 dG_s/dn_s + n_s d^2 G_s/dn_s^2) \\
&\quad + (1/16)(16 + 9\pi) (2 dG_s/dn_s + n_s d^2 G_s/dn_s^2), \\
\frac{d^2 G_s}{dn_s^2} &= (9\pi^2/2) (75 + \sqrt{3}\pi n_s) (6 - \sqrt{3}\pi n_s)^{-4}.
\end{aligned}$$

We have denoted for brevity $a_0 = T_s^{1/2}(x)$, $a_1 = a_0'$ and $a_2 = a_0''$. The boundary conditions for the functions Θ and ψ are the following:

$$\Theta(\pm 1/2) = \psi(\pm 1/2) = 0. \tag{7}$$

Equations (5)-(7) define a linear *boundary-value* problem: there are two boundary conditions at one wall, and two at the other wall. A simple and accurate numerical algorithm, that we

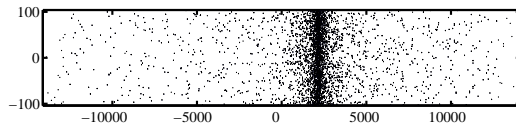


Fig. 2 – A snapshot of the system of $N = 3390$ inelastic hard disks within the instability region, obtained in a MD simulation. The left and right walls are thermal walls. The coefficient of normal restitution $r = 0.85$. See the text for the rest of the parameters. A large deviation of the cluster from the center of the system $x = 0$ is clearly seen.

developed earlier [24], enables one to avoid the unpleasant shooting in two parameters. The algorithm yields the complex value of ω . Varying R at fixed f and ϵ , we determined the critical value $R = R_c$ for the instability onset from the condition $\text{Im}\omega = 0$. The instability occurs at $R > R_c$. Given the rest of the parameters, the instability occurs when q exceed a critical value. Importantly, the instability is *oscillatory*, as $\text{Re}\omega \neq 0$ at the onset. Figure 1b shows the critical value $R = R_c$ versus the average area fraction f at a fixed ϵ .

MD simulations. – To verify the hydrodynamic predictions, and to follow the dynamics of an oscillating stripe in a nonlinear regime, we performed MD simulations with $N = 3390$ inelastic hard disks with unit mass and diameter. As Fig. 1b shows, the oscillatory instability region lies within the spinodal interval of the phase separation instability [11,13,14]. The phase separation instability is suppressed when the aspect ratio H/L is less than some threshold value depending on R [11,12,13]. It has been found recently that the system exhibits large fluctuations even well below the threshold [16]. Therefore, to isolate the oscillatory instability from the phase separation instability, we worked with a very small aspect ratio: the box dimensions were $H = 208$ and $L = 28\,209$. The parameters $f = 5 \cdot 10^{-4}$ and $\epsilon = 4 \cdot 10^{-5}$ were fixed. The parameter R varied from $4.42 \cdot 10^8$ to $9.55 \cdot 10^6$. This was achieved by varying r from 0.85 to 0.997. We employed the event-driven algorithm described in the book of Rapaport [25]. Upon collision with a thermal wall, the normal component of the particle velocity was drawn from a Maxwell distribution with $T_0 = 1$, while the tangential component of the velocity remained unchanged. The initial spatial distribution of the particles was uniform; the initial velocity distribution was Maxwell's with $T_0 = 1$. Figure 2 shows a typical snapshot of the

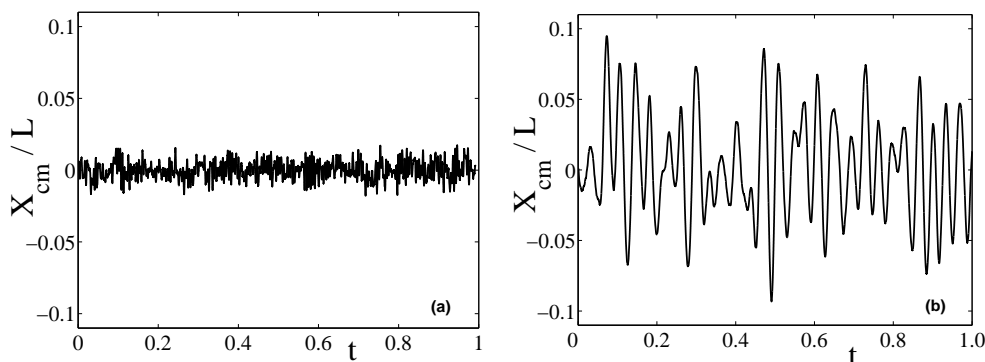


Fig. 3 – The time dependence of the center-of-mass coordinate X_{cm} , obtained in MD simulations with $N = 3390$ particles within (a) stable region, $r = 0.997$ and (b) unstable region, $r = 0.85$. The time unit is $10^7 t_{MD}$, where $t_{MD} = d/T_0^{1/2} = 1$.

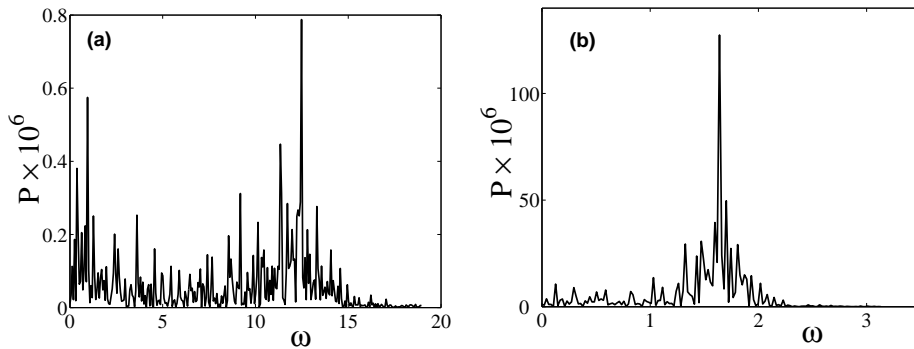


Fig. 4 – The power spectra within the stable (a) and unstable (b) regions. The frequency unit is $2\pi \cdot 10^{-5}$. The parameters in Figs. a and b are the same as in Figs. 3a and 3b, respectively. Notice the large differences in scales.

system obtained in a MD simulation within the instability region. A large deviation of the cluster from the center of the system $x = 0$ is clearly seen. A movie of this simulation can be seen at <http://huji-phys.phys.huji.ac.il/staff/Khain/abstract.html>. The oscillatory motion of the cluster was monitored by following the x -component of the center of mass of all particles, X_{cm} , versus time. Figure 3 shows this dependence as observed in the stable (a) and unstable (b) regions. The large-amplitude low-frequency irregular oscillations in the unstable case are clearly distinguishable from the small-amplitude high-frequency noise observed in the stable region. The power spectra for these two cases are shown in Fig. 4. Notice the large difference in scale in the horizontal axes and the huge difference in the vertical axes. In contrast to the low-amplitude noise of Fig. 4a, the power spectrum within the instability region (Fig. 4b) has a sharp peak at a single frequency $1.03 \cdot 10^{-4}$. This frequency is fairly close (within 30%) to the hydrodynamic frequency at the instability onset which, in the units of $t_{MD}^{-1} = 1$, is $1.45 \cdot 10^{-4}$. These two frequencies are not expected to *coincide*. Firstly, the steady-state oscillations, observed in the MD simulation (Figs. 3b and 4b), must be affected by hydrodynamic nonlinearities that are neglected in the linear stability analysis. Secondly, the next-order corrections in q can become significant at the moderate value of $r = 0.85$ used in this simulation [22].

The presence of a significant continuum part in the power spectrum of $X_{cm}(t)$ in Fig. 4b clearly shows that the cluster oscillations are chaotic. The same conclusion follows from the analysis of the phase trajectory in the phase plane (X_{cm}, \dot{X}_{cm}) . The chaotic component of the oscillations is due to irregular *cluster* motion, not due to the dynamics of the surrounding gas. We double-checked it by following the position X_* of the maximum number density of the system (integrated over the y -direction) versus time. The graph of $X_*(t)$ almost coincides with the graph of $X_{cm}(t)$; the respective power spectra are almost indistinguishable. Obviously, the chaotic component of the cluster oscillations is completely missed by the linear stability analysis. Furthermore, hydrodynamics predicts, at fixed f and ϵ , a sharp instability onset at $R = R_c$. On the contrary, a fairly smooth transition is observed in MD simulations. We believe it is due to the relatively small number of particles that causes significant fluctuations and smoothes the transition [26]. These fluctuations make it difficult to verify the reentrant behavior (see the right branch of the solid line in Fig. 1b) predicted by hydrodynamics.

Summary and Discussion. – We have discovered a new oscillatory instability in a system of inelastically colliding hard spheres, driven by two opposite “thermal” walls at zero gravity.

The instability has a hydrodynamic character and can therefore be interpreted in terms of the collective modes of the system. There are three such modes, coupled due to the inhomogeneity of the unperturbed state of the system. Two of the modes are oscillatory acoustic modes, the third one is a non-oscillatory entropy mode (the fourth, shear mode, is suppressed because of the very small aspect ratio of the box). It is the acoustic modes that become unstable at $R > R_c$. To some extent, this instability is similar to the acoustic instability (the so called "overstability") found in externally heated and radiatively cooling optically thin plasmas [19]. The future work should address the nonlinear regime of the cluster oscillations and clarify the role of discrete-particle noise versus the spatio-temporal chaos caused by hydrodynamic nonlinearities.

* * *

E.K. is very grateful to D.C. Rapaport for guidance in MD simulations. We thank P. V. Sasorov for a useful discussion. The work was supported by the Israel Science Foundation (grant No. 180/02).

REFERENCES

- [1] *Granular Gases*, edited by PÖSCHEL T. and LUDING S. (Springer, Berlin) 2001; *Granular Gas Dynamics*, edited by PÖSCHEL T. and BRILLIANTOV N. (Springer, Berlin) 2003; GOLDBIRSCHE I., *Annu. Rev. Fluid Mech.*, **35** (2003) 267.
- [2] GOLDBIRSCHE I. and ZANETTI G., *Phys. Rev. Lett.*, **70** (1993) 1619; MCNAMARA S. and YOUNG W. R., *Phys. Rev. E*, **53** (1996) 5089; DELTOUR P. and BARRAT J. L., *J. Phys. I. France*, **7** (1997) 137; VAN NOIJE T. P. C., ERNST M. H., BRITO R. and ORZA J. A. G., *Phys. Rev. Lett.*, **79** (1997) 411; BRITO R. and ERNST M. H., *Europhys. Lett.*, **43** (1998) 497; LUDING S. and HERRMANN H. J., *Chaos*, **9** (1999) 673; NIE X. B., BEN-NAIM E. and CHEN S. Y., *Phys. Rev. Lett.*, **89** (2002) 204301.
- [3] DU Y., LI H. and KADANOFF L. P., *Phys. Rev. Lett.*, **74** (1995) 1268.
- [4] KUDROLLI A., WOLPERT M. and GOLLUB J. P., *Phys. Rev. Lett.*, **78** (1997) 1383.
- [5] GROSSMAN E. L., ZHOU T. AND BEN-NAIM E., *Phys. Rev. E*, **55** (1997) 4200.
- [6] ESIPOV S. E. and PÖSCHEL T., *J. Stat. Phys.*, **86** (1997) 1385.
- [7] OLAFSEN J. S. and URBACH J. S., *Phys. Rev. Lett.*, **81** (1998) 4369; NIE X. B., BEN-NAIM E. and CHEN S. Y., *Europhys. Lett.*, **51** (2002) 679; CAFIERO R., LUDING S. and HERRMANN H. J., *Phys. Rev. Lett.*, **84** (2000) 6014.
- [8] BREY J. J. and CUBERO D., *Phys. Rev. E*, **57** (1998) 2019.
- [9] EGGERS J., *Phys. Rev. Lett.*, **83** (1999) 5322; VAN DER WEELE K., VAN DER MEER D., VERSLUIS M. and LOHSE D., *Europhys. Lett.*, **53** (2001) 328.
- [10] TOBOCHNIK J., *Phys. Rev. E*, **60** (1999) 7137.
- [11] LIVNE E., MEERSON B. and SASOROV P. V., *Phys. Rev. E*, **65** (2002) 021302.
- [12] BREY J. J., RUIZ-MONTERO M. J., MORENO F. and GARCIA-ROJO R., *Phys. Rev. E*, **65** (2002) 061302.
- [13] KHAIN E. and MEERSON B., *Phys. Rev. E*, **66** (2002) 021306.
- [14] ARGENTINA M., CLERC M. G. and SOTO R., *Phys. Rev. Lett.*, **89** (2002) 044301.
- [15] LIVNE E., MEERSON B. and SASOROV P. V., *Phys. Rev. E*, **66** (2002) 050301(R).
- [16] MEERSON B., PÖSCHEL T., SASOROV P.V. and SCHWAGER T., e-print cond-mat/0208286.
- [17] KHAIN E., MEERSON B. and SASOROV P. V., in preparation.
- [18] BLAIR D. L. and KUDROLLI A., *Phys. Rev. E*, **67** (2003) 041301.
- [19] FIELD G. B., *Astrophys. J.*, **142** (1965) 531; MEERSON B., *Rev. Mod. Phys.*, **68** (1996) 215.
- [20] HAFF P. K., *J. Fluid Mech.*, **134** (1983) 401.
- [21] JENKINS J. T. and RICHMAN M. W., *Phys. Fluids*, **28** (1985) 3485.

- [22] A more complete theory should include corrections of the order of q to the constitutive relations, as well as a *density* gradient term, also of the order of q , in the heat flux [23]. In the nearly-elastic limit $q \ll 1$ that we consider in our hydrodynamic analysis, these corrections can be neglected.
- [23] BREY J. J., DUFTY J. W., KIM C. S. and SANTOS A., *Phys. Rev. E*, **58** (1998) 4638.
- [24] KHAIN E. and MEERSON B., *Phys. Rev. E*, **67** (2003) 021306.
- [25] RAPAPORT D. C., *The Art of Molecular Dynamics Simulation* (Cambridge University Press, Cambridge) 1995.
- [26] HAKEN H., *Synergetics* (Springer, Berlin) 1978.